

SPECIAL ISSUE PAPER

# Sorghum stay-green QTL individually reduce post-flowering drought-induced leaf senescence

Karen Harris<sup>1</sup>, P. K. Subudhi<sup>2</sup>, Andrew Borrell<sup>3,\*</sup>, David Jordan<sup>3</sup>, Darrell Rosenow<sup>4</sup>, Henry Nguyen<sup>5</sup>, Patricia Klein<sup>6</sup>, Robert Klein<sup>7</sup> and John Mullet<sup>1</sup>

<sup>1</sup> Department of Biochemistry and Biophysics, Texas A&M University, College Station, Texas 77843, USA

<sup>2</sup> Molecular Genetics and Plant Genomics Laboratory, Department of Plant and Soil Science, Texas Tech University, Lubbock, Texas 79409-2122, USA

<sup>3</sup> Department of Primary Industries and Fisheries, Hermitage Research Station, Warwick, Queensland 4370, Australia

<sup>4</sup> Texas A&M University Agricultural Research and Extension Center, Lubbock, Texas 79401, USA

<sup>5</sup> Division of Plant Sciences and Center for Soybean Biotechnology, University of Missouri-Columbia, Columbia, Missouri 65211, USA

<sup>6</sup> Department of Horticultural Sciences and Institute for Plant Genomics and Biotechnology, Texas A&M University, College Station, Texas 77843, USA

<sup>7</sup> USDA-ARS, Southern Plains Agricultural Research Center, College Station Texas 77845, USA

Received 23 December 2005; Accepted 9 October 2006

## Abstract

Sorghum is an important source of food, feed, and biofuel, especially in the semi-arid tropics because this cereal is well adapted to harsh, drought-prone environments. Post-flowering drought adaptation in sorghum is associated with the stay-green phenotype. Alleles that contribute to this complex trait have been mapped to four major QTL, *Stg1–Stg4*, using a population derived from BT×642 and RT×7000. Near-isogenic RT×7000 lines containing BT×642 DNA spanning one or more of the four stay-green QTL were constructed. The size and location of BT×642 DNA regions in each RT×7000 NIL were analysed using 62 DNA markers spanning the four stay-green QTL. RT×7000 NILs were identified that contained BT×642 DNA completely or partially spanning *Stg1*, *Stg2*, *Stg3*, or *Stg4*. NILs were also identified that contained sub-portions of each QTL and various combinations of the four major stay-green QTL. Physiological analysis of four RT×7000 NILs containing only *Stg1*, *Stg2*, *Stg3*, or *Stg4* showed that BT×642 alleles in each of these loci could contribute to the stay-green phenotype. RT×7000 NILs containing BT×642 DNA

corresponding to *Stg2* retained more green leaf area at maturity under terminal drought conditions than RT×7000 or the other RT×7000 NILs. Under post-anthesis water deficit, a trend for delayed onset of leaf senescence compared with RT×7000 was also exhibited by the *Stg2*, *Stg3*, and *Stg4* NILs, while significantly lower rates of leaf senescence in relation to RT×7000 were displayed by all of the *Stg* NILs to varying degrees, but particularly by the *Stg2* NIL. Greener leaves at anthesis relative to RT×7000, indicated by higher SPAD values, were exhibited by the *Stg1* and *Stg4* NILs. The RT×7000 NILs created in this study provide the starting point for in-depth analysis of stay-green physiology, interaction among stay-green QTL and map-based cloning of the genes that underlie this trait.

Key words: Drought adaptation, NIL, sorghum, stay-green QTL.

## Introduction

Sorghum [*Sorghum bicolor* (L.) Moench] is the fifth most important cereal crop world-wide (<http://apps.fao.org/>

\* To whom correspondence should be addressed. E-mail: andrew.borrell@dpi.qld.gov.au

default.jsp) as well as an important source of feed, fibre, and biofuel (Doggett, 1988). Sorghum, like maize and sugarcane, carries out  $C_4$  photosynthesis, a specialization that makes these grasses well adapted to environments subject to high temperature and water limitation (Edwards *et al.*, 2004). Sorghum is an important target of genome analysis among the  $C_4$  grasses because the sorghum genome is relatively small ( $\sim 818$  Mbp) (Price *et al.*, 2005), the cultivated species is diploid ( $2n=20$ ) and the sorghum germplasm is diverse (Dje *et al.*, 2000; Menz *et al.*, 2004; Casa *et al.*, 2005). As a consequence, numerous sorghum genetic, physical, and comparative maps have been constructed (Tao *et al.*, 1998; Boivin *et al.*, 1999; Peng *et al.*, 1999; Klein *et al.*, 2000, 2003; Haussmann *et al.*, 2002a; Menz *et al.*, 2002; Bowers *et al.*, 2003, 2005), a sorghum EST project (Pratt *et al.*, 2005) and associated microarray analyses of sorghum gene expression have been carried out (Buchanan *et al.*, 2005; Salzman *et al.*, 2005), and a comprehensive analysis of sorghum chromosome architecture has been completed (Kim *et al.*, 2005). This genome infrastructure has enabled map-based cloning of *Rfl* (Klein *et al.*, 2005) and analysis of genes that control other important sorghum traits (Lin *et al.*, 1995; Pereira and Lee, 1995; Childs *et al.*, 1997; Tao *et al.*, 2003).

Sorghum is better adapted to water-limiting environments compared with most other crops (see reviews by Doggett, 1988; Ludlow and Muchow, 1990; Mullet *et al.*, 2001; Sanchez *et al.*, 2002). This attribute is of great importance as the demand for food and water supplies increases due to world population growth (Khush, 1999; Gleick, 2003). Two distinct drought-stress responses have been identified in sorghum (Rosenow and Clark, 1981, 1995; Rosenow, 1983): a pre-flowering drought response that occurs prior to anthesis and a post-flowering drought response that is observed when water limitation occurs during the grain-filling stage. Symptoms of post-flowering drought-stress susceptibility include premature leaf and plant senescence, stalk lodging and charcoal rot, and a reduction in seed size (Rosenow and Clark, 1995). Sorghum genotypes that exhibit resistance to pre-flowering and/or post-flowering drought have been identified (see review by Rosenow and Clark, 1995). Genotypes resistant to post-flowering drought stress were called 'stay-green' types because these plants retain chlorophyll in their leaves and maintain the ability to carry out photosynthesis longer than 'senescent' genotypes under terminal drought conditions. This phenotype is distinct from 'cosmetic' stay-green, which is characterized by senescing leaves that retain chlorophyll but lose the capacity to carry out photosynthesis (see reviews by Thomas and Smart, 1993; Thomas and Howarth, 2000; Cha *et al.*, 2002). The stay-green genotypes also exhibit reduced stalk lodging (Woodfin *et al.*, 1998) and resistance to charcoal rot (Rosenow, 1983).

The physiological basis of the sorghum stay-green trait remains to be clarified. Stay-green genotypes have been found to contain higher cytokinin levels (McBee, 1984; Ambler *et al.*, 1987) and more stem sugars (Duncan *et al.*, 1981; McBee and Miller, 1982; Dahlberg, 1992) than senescent genotypes under certain conditions. In addition, stay-green hybrids assimilate more nitrogen and have higher specific leaf nitrogen than senescent hybrids, suggesting a link between nitrogen status and the stay-green trait (Borrell and Hammer, 2000; Borrell *et al.*, 2001). However, it is unclear if these traits are a cause or a consequence of the stay-green trait, or are secondary traits that are associated with the general adaptation of stay-green genotypes to their agro-ecological zones. While the precise physiological basis of stay-green remains unclear, the positive impact of this trait on yield under terminal drought has been confirmed in several studies (Borrell *et al.*, 2000b; Jordan *et al.*, 2003). Moreover, this trait has little, if any, yield penalty when plants are grown under conditions where water is not limiting (Borrell *et al.*, 2000b).

Several sorghum genotypes have been identified that exhibit the stay-green trait (BT $\times$ 642, SC56, E36-1) (Rosenow, 1983; Kebede *et al.*, 2001; Haussmann *et al.*, 2002b). The genotype BT $\times$ 642 (formerly B35) has been an especially useful source of stay-green for research (Tuinstra *et al.*, 1997, 1998; Crasta *et al.*, 1999; Subudhi *et al.*, 2000; Tao *et al.*, 2000; Xu *et al.*, 2000) and the development of commercial hybrids (Henzell *et al.*, 2001). BT $\times$ 642 is derived from IS12555, a durra sorghum from Ethiopia. Genetic studies showed that the BT $\times$ 642 genes conferring the stay-green trait act with varied levels of dominance (Walulu *et al.*, 1994) or an additive fashion if the onset of senescence was analysed (van Oosterom *et al.*, 1996). Several stay-green QTL mapping studies have been conducted using BT $\times$ 642 as one of the parents (Tuinstra *et al.*, 1996, 1997, 1998; Crasta *et al.*, 1999; Subudhi *et al.*, 2000; Tao *et al.*, 2000; Xu *et al.*, 2000). These studies identified four major QTL designated *Stg1*, *Stg2*, *Stg3*, and *Stg4* and many additional minor QTL that can modulate expression of the stay-green trait. *Stg1* and *Stg2* were located on LG-03 and explained  $\sim 20\%$  and  $\sim 30\%$  of the phenotypic variability, respectively (Xu *et al.*, 2000; Sanchez *et al.*, 2002). *Stg3* was located on LG-02 and *Stg4* on LG-05, accounting for  $\sim 16\%$  and  $\sim 10\%$  of the phenotypic variance, respectively (Sanchez *et al.*, 2002). The ranking of stay-green QTL based on their contribution to the stay-green phenotype in the BT $\times$ 642 by RT $\times$ 7000 population is *Stg2* $>$ *Stg1* $>$ *Stg3* $>$ *Stg4* (Xu *et al.*, 2000). In relatively small RIL populations such as those that have been used for mapping stay-green, the influence of an individual QTL on expression of the phenotype can be difficult to quantify because (i) the experiments have limited statistical power to detect QTL (Beavis, 1994; Melchinger *et al.*, 1998), (ii) detection may be influenced by G $\times$ E interactions and genetic

background effects (Tuinstra *et al.*, 1998), and (iii) the effects of the QTL that are detected tend to be biased upwards (Beavis, 1994; Melchinger *et al.*, 1998).

A number of epistatic interactions among stay-green loci and between stay-green loci and genes in other regions of the sorghum genome have been identified (Subudhi *et al.*, 2000). Near-isogenic lines (NILs) can be used to help clarify complex genetic interactions and phenotypes such as those associated with the stay-green trait. For example, 14 QTL were found to regulate flowering time in a cross of *O. sativa japonica* and *O. sativa indica*. Three flowering time QTL, *Hd1*, *Hd3a*, and *Hd6* were fine mapped using NIL-derived material and the corresponding genes subsequently isolated using a map-based cloning approach (Paran and Zamir, 2003). Therefore, this approach was adopted to facilitate the physiological and genetic analysis of the genes that modulate the stay-green trait associated with BT×642. During the course of these studies, 34 RT×7000 NILs were developed by crossing BT×642 with the senescent genotype RT×7000 followed by subsequent introgression of one or more of the BT×642 stay-green QTL regions into the RT×7000 background. NILs containing *Stg1*, 2, 3, and 4 were identified and found to have enhanced stay-green related phenotypes relative to RT×7000.

## Materials and methods

### Generation of RT×7000 NILs containing BT×642 DNA from the stay-green loci

Near-isogenic RT×7000 lines containing one or more of the *Stg* loci from BT×642 were constructed starting with a cross of BT×642 and RT×7000 followed by repeated backcrossing of F<sub>1</sub>

plants to RT×7000 either four (6000 NIL series) or six times (2000 NIL series) (Fig. 1).

Progeny derived from each backcross were screened for one or more of the *Stg* loci using DNA markers that mapped within or near each locus (Fig. 2; DNA markers with arrows). For example, progeny containing BT×642 DNA spanning *Stg1* were identified using the markers *NPI414*, *Xtxs1114*, and *BNL15.20* (Fig. 2; markers in bold with arrows to the right). As a consequence several RT×7000 NILs were generated that contain a block of BT×642 DNA spanning *Stg1* (Fig. 2, NILs 6078-1, 6086-3, 6102-23, 6100-7). Similarly, NILs containing BT×642 DNA corresponding to *Stg2*, *Stg3*, and/or *Stg4* were generated using *Xtxs584*, *RZ323*, *CSU58*, *A12-420* (*Stg2*), *Xtxs1307*, *Xtxs1111*, *UMC5* (*Stg3*), and *Xtxs713* (*Stg4*) (Fig. 2). Selection was continued until the BC<sub>4</sub> or BC<sub>6</sub> generation where the lines were selfed to create BC<sub>4</sub>F<sub>2-4</sub> or BC<sub>6</sub>F<sub>2-4</sub> lines.

### DNA extraction and DNA marker analysis

Genomic DNA of IS3620C, BT×623, BT×642, and RT×7000 was extracted from sorghum leaf tissue with a FastDNA kit using a FastPrep FP120 homogenizer according to the manufacturer's instructions (Qbiogene, Irvine, CA, USA). DNA was purified using a GENECLEAN Turbo kit (Qbiogene). AFLP template was prepared according to Vos *et al.* (1995), using the restriction enzymes *EcoRI* and *MseI*. DNA template preparation, amplification and visualization of amplified AFLP products were performed as described by Klein *et al.* (2000). The following *EcoRI* and *MseI* primer combinations were used for AFLP analysis: E-ACC+M-CGG, E-ACC+M-CTA, E-ACC+M-CTC, E-AGT+M-CTA, E-AGT+M-CTG, E-CTG+M-CAC, E-CTG+M-CCC, E-CTG+M-CTG, E-GAA+M-CAA, E-GAA+M-CAT, E-GAA+M-CCG, E-GAA+M-CTG, E-GGA+M-CAA, E-GGA+M-CAG, E-GGA+M-CTC, E-TAC+M-CTT, E-TGA+M-CCT, E-TGA+M-CTA, and E-TGA+M-CTG.

SSRs were amplified and analysed using fluorescent IRD-labelled primers obtained from Li-Cor (Lincoln, NE, USA) as described by Klein *et al.* (2000) or 5' HEX (IDT, Coralville, IA, USA) forward-labelled primers. PCR reaction conditions were identical for both primer substrates, except that the concentrations of forward and reverse primers were 2.5 pmol μl<sup>-1</sup> for HEX-labelled primers and 1 pmol μl<sup>-1</sup> for IRD-labelled primers. Data were analysed with

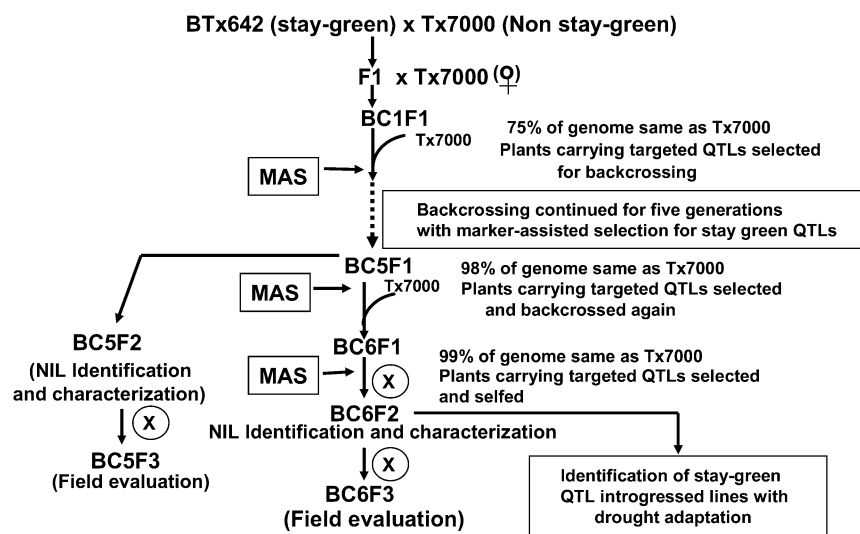
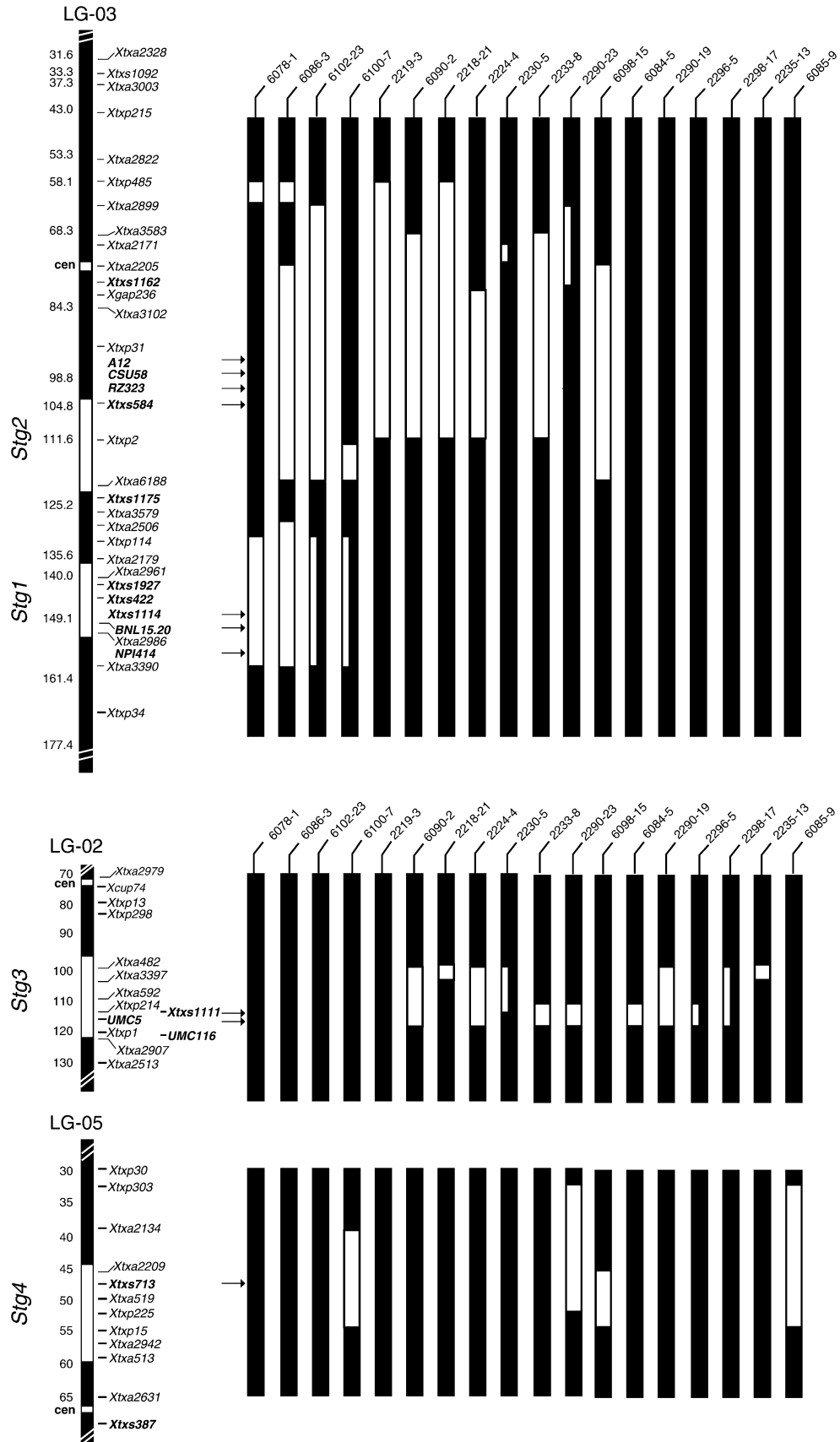


**Fig. 1.** Scheme for developing near-isogenic lines (NILs) for stay-green QTLs using marker-assisted selection (MAS) (modified from Subudhi *et al.*, 1999, and reproduced by kind permission of the International Rice Research Institute).



Gene Scan version 3.7 Fragment Analysis Software (Applied Biosystems, Foster City, CA, USA) and peaks were scored manually using the Genotyper version 3.7 Fragment Analysis Software (Applied Biosystems). SSR primer sequences and amplification product sizes are listed at <http://sorgblast2.tamu.edu/>. Sixty-two of the 113 AFLP and SSR markers analysed mapped within one of the stay-green QTL. Markers outside these regions were also analysed to provide a random background survey of NIL genotypes.

#### Screening RT×7000 NILs for the stay-green phenotype

Four of the RT×7000 NILs contained BT×642 DNA spanning all, or a portion, of only *Stg1*, *Stg2*, *Stg3*, or *Stg4*. These NILs were targeted for further physiological analysis to determine if the BT×642 DNA introgressed into each of these NILs contained genes that would contribute to the stay-green trait independent of the other *Stg* loci.

Field experiments to characterize the NILs physiologically were conducted at the Hermitage Research Station (altitude 480 m, 28°10' S, 152°02' E) in Australia's north-eastern grain belt in two consecutive seasons: Experiment 1 (2004) and Experiment 2 (2005). Both experiments consisting of the *Stg* NILs and RT×7000 were grown at a rain-out shelter facility on a cracking and weakly self-mulching brownish-black clay (Talgai shallow phase; McKeown, 1978; Ug 5.14; Northcote, 1974). The experiment site has a slope of about 2% and the profile is moderately well drained. The experiment design was a randomized split block, with two density treatments (main plots) split by different genotypes (subplots). The experiments were replicated four times. Fertilizers were applied so that crop growth was not limited by nutrients in either treatment. Main plots were 3 m×12.5 m and subplots were 2 m (4 rows)×3 m. The main treatments were high density (20 plants m<sup>-2</sup>; HD) and low density (10 plants m<sup>-2</sup>, LD). Irrigation was applied to both treatments until 16 (Experiment 1) and 24 (Experiment 2) days before anthesis, after which time no more water was applied, creating a terminal water deficit. Terminal stress typifies the dry season of the semiarid tropics, where crops are usually grown solely on stored soil moisture in heavy soils, with the crop maturing progressively on a depleted soil moisture profile. The severity of drought was greater in Experiment 1 than in Experiment 2, due to earlier planting of the experiment in the 2004 season (11 December 2003) compared with the 2005 season (21 January 2005). Five of the six genotypes will be discussed in this paper: 6078-1 (*Stg1* NIL), 2219-3 (*Stg2* NIL), 2290-19 (*Stg3* NIL), 6085-9 (*Stg4* NIL), and RT×7000 (recurrent parent). The *Stg4* NIL (6085-9) was grown only in Experiment 2.

Absolute rate of leaf senescence was calculated as the slope of the linear decline over time from anthesis to maturity (cm<sup>2</sup> m<sup>-2</sup> d<sup>-1</sup>). Relative rate of leaf senescence was calculated from the slope of the linear decline over time from anthesis to maturity of green leaf area, relative to green leaf area at anthesis, expressed as the loss of relative leaf area (% d<sup>-1</sup>): [(1-GLAM/GLAA)×100]/days from anthesis to maturity, where GLAM is the green leaf area at maturity (cm<sup>2</sup> m<sup>-2</sup>) and GLAA is the green leaf area at anthesis (cm<sup>2</sup> m<sup>-2</sup>).

In addition, leaf greenness, an integrated measure of the stay-green phenotype, was recorded on the leaf below the flag (FL-1) throughout the grain-filling period in the 2005 season. A Minolta chlorophyll meter (SPAD-502) was used to measure the greenness of FL-1 from four tagged plants in each plot at weekly intervals. Three measurements were taken down one side of the leaf at the base, centre and tip, approximately 1 cm from the leaf edge. Broken-stick functions were fitted to the individual plot data for the SPAD regression on time (d) and the following coefficients were determined:

a=value of the asymptote (benchmark of leaf greenness at anthesis);

b=slope of the first linear phase of the broken-stick function (fixed at zero);

c=slope of the second linear phase of the broken-stick function (rate of decline in SPAD with senescence); and

d=intersection of the two linear phases of the broken-stick function (onset of leaf senescence).

Leaf greenness at maturity ( $SPAD_m$ ) can be described mathematically by adapting 'Equation 4' from Borrell *et al.* (2000a), initially used to estimate green leaf area at maturity:

$$SPAD_m = SPAD_a - (Duration_{sen} \times Rate_{sen})$$

where  $SPAD_a$  is the 'benchmark' leaf greenness prior to the commencement of senescence (initial asymptote corresponding to coefficient 'a' in the broken-stick function),  $Duration_{sen}$  is the duration of leaf senescence (d) between the onset of senescence (coefficient 'd' in the broken-stick function) and physiological maturity, and  $Rate_{sen}$  is the rate of leaf senescence (loss of  $SPAD$  d<sup>-1</sup>) determined by the slope of the second linear phase of the broken-stick function (coefficient 'c'). Onset of leaf senescence was estimated as the time at which the two linear phases of the  $SPAD$  function intersected.

#### Statistical analyses associated with phenotyping

The data were analysed using linear mixed models including fixed treatment terms (plant density, genotype, and their interaction) and random terms to reflect the blocking structure of the design (replicate, mainplot, subplot, and the appropriate interactions between these terms). In addition, the model accommodated error variance heterogeneity between the rain-out shelters.

## Results

### Aligning stay-green loci mapped in BT×642/RT×7000 to the BT×623/IS3620C genetic map

Xu *et al.* (2000) utilized 98 F<sub>7</sub> RIL lines derived from a cross of BT×642 and RT×7000 to map four major

**Fig. 2.** Size and location of BT×642 DNA introgressions in RT×7000 NILs. A portion of the three sorghum linkage groups (defined by Kim *et al.*, 2005) that span *Stg1*–*Stg4* (shaded white) are shown at the left of the figure. The DNA markers used for analysis are listed to the right of each linkage group with lines indicating their approximate location (relative map location is indicated in cM to the left of each linkage group). The approximate location of the centromeres relative to each linkage map is noted by a white square marked CEN. A subset of the DNA markers in bold was used to align the genetic map based on BT×642/RT×7000 and BT×623/IS3620C (*BNL15.20*, *Xtxs422*, *Xtxs1927*, *Xtxs1175*, *Xtxs584*, *Xtxs1111*, *UMC5*, *UMC116*, *Xtxs387*, and *Xtxs713*). DNA markers in bold with arrows to the right were used during construction of the RT×7000 NILs to select lines containing BT×642 introgressions. The genotype of RT×7000 NILs is shown to the right where black indicates RT×7000 DNA and white represents BT×642 DNA. White bars that are half the width of each linkage group represent heterozygous blocks of DNA. NILs with similar patterns of BT×642 DNA introgression are shown only once (2208-12=2209-4, 2219-3, 2219-8; 6090-2=2223-3, 2226-11, 2234-8, and 2289-20; 6084-5=2293-12, 2289-19; 6083-1=2229-5). Markers without a tick mark were placed on the TAMU-ARS map based on the results of Subudhi *et al.* (2000).

stay-green loci segregating in this population. The stay-green loci were located on a genetic map that spanned ~837 cM based on the analysis of 162 RFLP markers (Xu *et al.*, 2000). To assist further analysis of the stay-green loci identified by Xu *et al.* (2000), the regions of the sorghum genome spanning *Stg1–Stg4* were located on the 1713 cM high density genetic map developed by Menz *et al.* (2002) based on 137 RILs derived from BT×623/IS3620C. There were several DNA markers located near or within the stay-green loci that were common to both genetic maps. For example, five DNA markers located near or within *Stg1* and *Stg2* on the BT×642/RT×7000 linkage map were located on LG-03 of the BT×623/IS3620C linkage map (Fig. 2; markers in bold; *Xtxs584*, *Xtxs1175*, *Xtxs422*, *Xtxs1927*, and *BNL15.20*). Similarly, several DNA markers spanning *Stg3* and *Stg4* on the BT×642/RT×7000 map were also located on the BT×623/IS3620C linkage map (Fig. 2, markers in bold; *Xtxs1162*, *Xtxs1111*, *UMC5*, *UMC116*, *Xtxs713*, and *Xtxs387*). Having aligned the two maps in the syntenic regions spanning *Stg1–Stg4*, additional information was collected to define the boundaries of each QTL on the BT×623/IS3620C map. The stay-green QTL were mapped in the BT×642/RT×7000 RIL population using phenotypic data collected from several geographical regions and in different years (Xu *et al.*, 2000). As a consequence, the size and location of the stay-green loci mapped in the different studies varied to some extent (Xu *et al.*, 2000). Due to this variation, a composite interval defined by all of the QTL studies was located on the BT×623/IS3620C map. The size and location of each stay-green QTL on the BT×623/IS3620C map was estimated based on DNA markers common to both maps, and the ratio of recombination observed between aligned regions of the two maps spanning the stay-green loci (Fig. 2; white regions labelled *Stg1–Stg4*). This analysis showed that each of the four stay-green loci spanned a maximum of ~10–30 cM on the BT×623/IS3620C map.

#### Generation of RT×7000 NILs containing BT×642 DNA from the stay-green loci

Near-isogenic RT×7000 lines containing one or more of the *Stg* loci from BT×642 were constructed starting with a cross of BT×642 and RT×7000 followed by repeated backcrossing of F<sub>1</sub> plants to RT×7000 either four (6000 NIL series) or six times (2000 NIL series) (Fig. 1). Thirty-four RT×7000 NILs were analysed using a total of 113 AFLP and SSR markers (Fig. 2). Sixty-two of the DNA markers used in the analysis were located either within or adjacent to each stay-green locus. This provided information on the size and location of the BT×642 DNA regions that had been introgressed into each RT×7000 NIL (Fig. 2, regions marked in white). Several NILs did not contain BT×642 DNA that overlapped with a stay-green QTL and

were eliminated from further analysis. In addition, several NILs had similar BT×642 introgression patterns, therefore, only one example of each of these NILs is shown in Fig. 2 (see figure legend). The patterns of BT×642 introgression in the resulting 18 NILs are shown in Fig. 2. Four NILs contained BT×642 DNA that spanned *Stg1* (Fig. 2, 6078-1, 6083-3, 6102-23, 6100-7). Among these NILs, 6078-1, designated a *Stg1* NIL, contained BT×642 DNA spanning *Stg1* but none of the other *Stg* loci. Nine NILs contained BT×642 DNA spanning nearly all or a subportion of the *Stg2* QTL (Fig. 2). *Stg2* NIL, 2219-3, contained BT×642 DNA that spanned most of the *Stg2* locus (~104.8 to ~111.6–118 cM) plus a region flanking the *Stg2* locus (~65 cM to ~104.8 cM) but none of the other *Stg* loci. A similar analysis identified 2290-19 as a *Stg3* NIL and 6085-9 as a *Stg4* NIL. Furthermore, several NILs were identified that contained BT×642 DNA that spanned all or a portion of two or more *Stg* loci (i.e. 6086-3=*Stg1+Stg2*; 6098-15=*Stg2+Stg4*). It was also noted that for a few NILs, DNA in some regions was heterozygous or heterogeneous (i.e. NIL 2230-5, *Stg3* region) (Fig. 2; marked by ½ width white bars).

#### Screening RT×7000 NILs for the stay-green phenotype

*Rate of leaf senescence:* Genotype×density interactions were not significant at  $P=0.05$  for the absolute rate of leaf senescence ( $aRATE_{sen}$ ) in Experiment 1 or 2 (Table 1). In Experiment 1,  $aRATE_{sen}$  was higher ( $P < 0.01$ ) in RT×7000 ( $715 \text{ cm}^2 \text{ m}^{-2} \text{ d}^{-1}$ ) than in *Stg2* ( $518 \text{ cm}^2 \text{ m}^{-2} \text{ d}^{-1}$ ) or *Stg3* ( $578 \text{ cm}^2 \text{ m}^{-2} \text{ d}^{-1}$ ) NILs. In Experiment 2,  $aRATE_{sen}$  was higher in RT×7000 ( $612 \text{ cm}^2 \text{ m}^{-2} \text{ d}^{-1}$ ) compared with all of the *Stg* NILs ( $Stg2=Stg3 > Stg4 > Stg1$ ).

No genotype×density interaction ( $P < 0.05$ ) was observed for the relative rate of leaf senescence ( $rRATE_{sen}$ ) in Experiment 1, although the interaction was significant ( $P < 0.01$ ) in Experiment 2. In Experiment 1,  $rRATE_{sen}$  was less in the *Stg2* NIL (2.01%) compared with RT×7000 (2.69%), and *Stg1* (2.58%) and *Stg3* (2.55%) NILs. In Experiment 2,  $rRATE_{sen}$  was less in *Stg2* (1.26%) and *Stg4* (1.26%) NILs compared with the *Stg3* NIL (1.38%) under HD, although none of the NILs was significantly different from RT×7000 (1.33%). However, under the LD treatment,  $rRATE_{sen}$  was higher in RT×7000 (1.36%) than in *Stg1* (1.14%) and *Stg2* (1.18%) NILs.

*Green leaf area at maturity (GLAM):* Genotype and density did not interact for *GLAM* in Experiment 1, although the interaction was significant ( $P < 0.01$ ) in Experiment 2 (Table 1). In Experiment 1, *GLAM* was higher in the *Stg2* NIL ( $6644 \text{ cm}^2 \text{ m}^{-2}$ ) compared with all other genotypes. There was, however, a trend for higher *GLAM* in *Stg1* ( $2125 \text{ cm}^2 \text{ m}^{-2}$ ) and *Stg3* ( $2112 \text{ cm}^2 \text{ m}^{-2}$ ) NILs compared with

**Table 1.** Absolute rate of leaf senescence, relative rate of leaf senescence, and green leaf area at maturity in *Stg* near-isolines and their recurrent parent (RT×7000) grown at two plant densities under a terminal post-anthesis water deficit in the 2004 (Experiment 1) and 2005 seasons (Experiment 2)

<i>Stg</i> region	Genotype	Main Effects			Genotype × treatment interactions					
		Absolute rate of leaf senescence (cm <sup>2</sup> m <sup>-2</sup> d <sup>-1</sup> )	Relative rate of leaf senescence (% loss LAI d <sup>-1</sup> )	Green leaf area at maturity (cm <sup>2</sup> m <sup>-2</sup> )	Absolute rate of leaf senescence (cm <sup>2</sup> m <sup>-2</sup> d <sup>-1</sup> )		Relative rate of leaf senescence (% loss LAI d <sup>-1</sup> )		Green leaf area at maturity (cm <sup>2</sup> m <sup>-2</sup> )	
Experiment 1 (2004 Season)										
					High density	Low density	High density	Low density	High density	Low density
<i>Stg1</i>	6078-1	619 bc <sup>a</sup>	2.58 b	2125 a	778 ab	459 ab	2.63 b	2.53 b	2106 a	2145 a
<i>Stg2</i>	2219-3	<b>518 a<sup>b</sup></b>	<b>2.01 a</b>	<b>6644 b</b>	<b>681 a</b>	<b>354 a</b>	<b>2.24 a</b>	<b>1.79 a</b>	<b>6445 b</b>	<b>6842 b</b>
<i>Stg3</i>	2290-19	<b>578 ab</b>	2.55 b	2112 a	<b>722 a</b>	433 ab	2.66 b	2.43 b	1878 a	2346 a
None	RT×7000	715 c	2.69 b	1292 a	866 b	564 b	2.78 b	2.60 b	859 a	1725 a
LSD ( <i>P</i> =0.05)		99	0.22	1456	140	140	0.31	0.31	2060	2060
<i>P</i> -value		0.003	<0.001	<0.001	0.068	0.068	0.13	0.13	0.243	0.243
Experiment 2 (2005 Season)										
					High density	Low density	High density	Low density	High density	Low density
<i>Stg1</i>	6078-1	<b>461 a</b>	<b>1.23 a</b>	<b>5901 bc</b>	478 ab	<b>444 a</b>	1.32 ab	<b>1.14 a</b>	3363 ab	<b>8440 b</b>
<i>Stg2</i>	2219-3	<b>509 a</b>	<b>1.22 a</b>	<b>6561 c</b>	537 ab	<b>480 a</b>	1.26 a	<b>1.18 a</b>	5765 b	<b>7356 b</b>
<i>Stg3</i>	2290-19	<b>509 a</b>	1.34 bc	2900 a	549 ab	<b>470 a</b>	1.38 b	1.29 b	2047 a	3753 a
<i>Stg4</i>	6085-9	<b>495 a</b>	<b>1.28 ab</b>	4420 ab	<b>455 a</b>	535 ab	1.26 a	1.30 b	4652 b	4188 a
None	RT×7000	612 b	1.35 c	3128 a	601 b	624 b	1.33 ab	1.36 b	3732 ab	2524 a
LSD ( <i>P</i> =0.05)		92	0.06	1719	130	130	0.08	0.08	2431	2431
<i>P</i> -value		0.016	<0.001	<0.001	0.423	0.423	0.003	0.003	0.006	0.006

<sup>a</sup> Means within a column not followed by a common letter are significantly different (*P*<0.05).<sup>b</sup> Values in bold are significantly different (*P*<0.05) from the recurrent parent (RT×7000).

**Table 2.** Components of SPAD at maturity in four *Stg* NILs and their recurrent parent (RT×7000) grown under a terminal post-anthesis water deficit in the 2005 season (Experiment 2)

<i>Stg</i> region	Genotype	SPAD at 67 DAA (measured)	SPAD at initial asymptote (coefficient 'a')	$Rate_{sen}$ Rate of loss of SPAD $d^{-1}$ (coefficient 'c')	Onset of senescence (days after anthesis) (coefficient 'd')	SPAD at 67 DAA (predicted by broken-stick function)
<i>Stg1</i>	6078-1	22.8 ab <sup>a</sup>	<b>56.7 c</b>	0.894 ab	27.1	21.6 ab
<i>Stg2</i>	2219-3	<b>28.9 b<sup>b</sup></b>	54.1 ab	0.760 a	31.8	<b>28.3 b</b>
<i>Stg3</i>	2290-19	17.1 a	54.7 abc	1.047 b	29.3	16.1 a
<i>Stg4</i>	6085-9	22.1 ab	<b>56.0 bc</b>	0.935 ab	28.5	21.4 ab
None	RT×7000	17.3 a	53.9 a	0.963 ab	26.8	16.0 a
LSD ( $P=0.05$ )		6.8	2.1	0.259	ns <sup>c</sup>	7.5
<i>P</i> -value	(genotype)	0.008	0.04	0.241	0.65	0.013
<i>P</i> -value	(interaction)	0.072	0.62	0.241	0.71	0.127

<sup>a</sup> Means within a column not followed by a common letter are significantly different ( $P<0.05$ ).

<sup>b</sup> Values in bold are significantly different ( $P<0.05$ ) from the recurrent parent (RT×7000).

<sup>c</sup> ns denotes F-test was not significant ( $P>0.05$ ).

RT×7000 (1292  $cm^2 m^{-2}$ ). In Experiment 2, RT×7000 was no different than any other genotype in *GLAM* under HD (3732  $cm^2 m^{-2}$ ), although there was a trend for lower *GLAM* in *Stg1* (3363  $cm^2 m^{-2}$ ) and *Stg3* (2047  $cm^2 m^{-2}$ ) NILs, and higher *GLAM* in *Stg2* (5765  $cm^2 m^{-2}$ ) and *Stg4* (4652  $cm^2 m^{-2}$ ) NILs, relative to RT×7000. Under LD, *GLAM* was higher in *Stg1* (8440  $cm^2 m^{-2}$ ) and *Stg2* (7356  $cm^2 m^{-2}$ ) NILs compared with RT×7000 (2524  $cm^2 m^{-2}$ ), with a trend for higher *GLAM* also observed for *Stg3* (3753  $cm^2 m^{-2}$ ) and *Stg4* (4188  $cm^2 m^{-2}$ ) NILs.

*Components of leaf greenness (Experiment 2 only):* The interactions between genotype and density were not significant at  $P=0.05$  for any of the components of leaf greenness, hence only main effect data will be presented (Table 2; Fig. 3). SPAD at 67 d after anthesis (DAA) on FL-1 was higher in the *Stg2* NIL (28.9) than in RT×7000 (17.3), although there was also a trend for higher leaf greenness in *Stg1* (22.8) and *Stg4* (22.1) NILs. Components of SPAD at 67 DAA (physiological maturity) were derived as coefficients of broken-stick functions fitted to regressions of SPAD on time (d) after anthesis (see Materials and methods for details). The observed SPAD values at 67 DAA were highly correlated ( $r^2=0.98$ ) with predicted SPAD values at 67 DAA ( $SPAD_m$ ) calculated using broken-stick functions (Fig. 4).  $SPAD_a$  at anthesis ( $SPAD_a$ ), the asymptote of the first linear phase of the broken-stick function (coefficient 'a'), represents the initial benchmark of leaf nitrogen prior to the commencement of senescence.  $SPAD_a$  was higher in *Stg1* (56.7) and *Stg4* (56.0) NILs compared with RT×7000 (53.9), with a trend for higher  $SPAD_a$  in the *Stg3* NIL (54.7). RT×7000 did not differ from any of the NILs in  $Rate_{sen}$  (0.96  $d^{-1}$ ), the rate of loss of SPAD  $d^{-1}$  following the onset of leaf senescence (coefficient 'c'). However, there was a trend for lower rates of senescence in *Stg1* (0.89  $d^{-1}$ ) and *Stg2* (0.76  $d^{-1}$ ) NILs. In fact, the  $Rate_{sen}$  observed in the *Stg2* NIL (0.76  $d^{-1}$ ) was significantly less

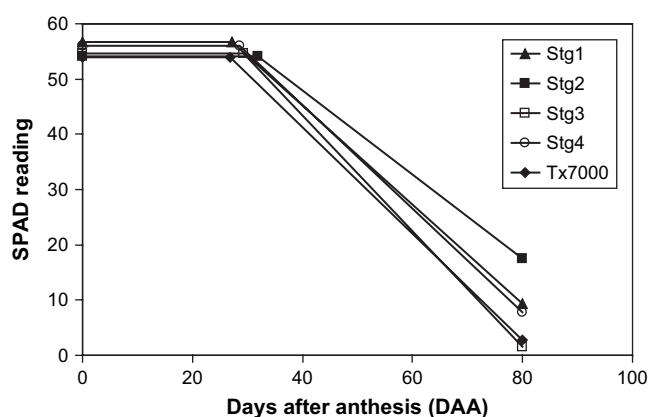


**Fig. 3.** Broken-stick functions fitted to regressions of SPAD versus time (d after anthesis, DAA) for four NILs (filled triangles, *Stg1*; filled squares, *Stg2*; open squares, *Stg3*; open circles, *Stg4*) and their recurrent parent (filled diamonds, RT×7000) grown under a terminal post-anthesis water deficit in the 2005 season (Experiment 2). The first linear phase of the broken-stick function (coefficient 'a') is the benchmark of leaf greenness (SPAD) at anthesis. The slope of the second linear phase (coefficient 'c') is the rate of decline of SPAD with senescence. Onset of leaf senescence (coefficient 'd') is defined as the time at which the two linear phases intersect.

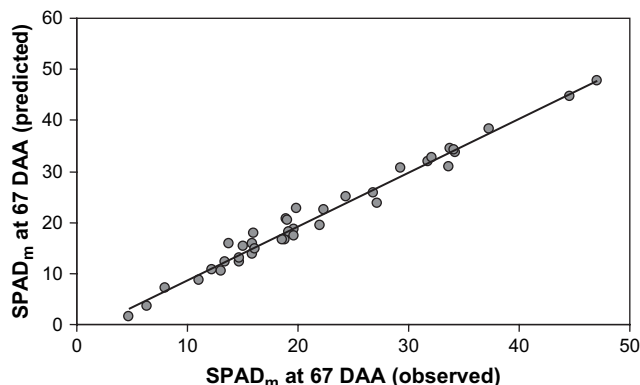


**Fig. 4.** The regression of observed  $SPAD_m$  values (FL-1) at 67 d after anthesis (DAA) versus the predicted values of  $SPAD_m$  at 67 DAA ( $R^2=0.98$ ) using coefficients derived from broken-stick functions in the 2005 season (Experiment 2).

than that observed for the *Stg3* NIL (1.05 d<sup>-1</sup>) in this parameter. Similarly, RT×7000 (26.8 DAA) did not vary from the NILs in onset of leaf senescence (coefficient 'd'), although a trend for delayed onset of senescence was observed in *Stg2* (31.8 DAA), *Stg3* (29.3 DAA), and *Stg4* (28.5 DAA) NILs. *SPAD<sub>m</sub>* was correlated with two of its components: coefficient 'a' (*SPAD* at anthesis,  $r=0.45$ ,  $n=40$ ,  $P<0.01$ ) and coefficient 'c' (rate of loss of *SPAD* d<sup>-1</sup>,  $r=-0.75$ ,  $n=40$ ,  $P<0.001$ ), but not with coefficient 'd' (onset of senescence,  $r=0.17$ ,  $n=40$ ).

## Discussion

The long-term goal of this research is to understand the physiological basis of the sorghum stay-green trait and to identify the genes that contribute to this trait in different sorghum genotypes. Prior studies on the BT×642 source of stay-green identified numerous QTL that modulate expression of the trait (Tuinstra *et al.*, 1997; Tao *et al.*, 2000; Xu *et al.*, 2000). Some of these QTL, such as *Stg1–Stg4*, are consistently expressed in a range of environments and in different genetic backgrounds (Tuinstra *et al.*, 1997; Crasta *et al.*, 1999; Subudhi *et al.*, 2000; Xu *et al.*, 2000). However, because the stay-green trait is expressed during grain-filling and involves leaf senescence, there are many secondary factors that can modulate this trait. For example, differences in flowering time and reproductive sink strength, in addition to variation in environmental factors, can influence expression of the stay-green trait (Rosenow and Clark, 1995). This complexity is consistent with our current understanding of the regulatory systems that modulate plant and leaf senescence now being revealed through genetic and genomic analyses (see reviews by Buchanan-Wollaston *et al.*, 2003; Yoshida, 2003). As a consequence, an in-depth analysis of the genetic and physiological basis of the sorghum stay-green trait requires the generation of a series of near-isogenic 'senescent' lines containing one or more of the stay-green loci.

This report describes the development of ~18 different RT×7000 BC<sub>4-6</sub>F<sub>2-4</sub> NILs that contain introgressed regions of BT×642 DNA. Detailed genetic analysis of the RT×7000 NILs showed that these lines contain BT×642 DNA spanning all or a portion of the four major stay-green loci, *Stg1–Stg4*, previously identified in a cross of RT×7000 and BT×642 (Subudhi *et al.*, 2000; Xu *et al.*, 2000). Several of the RT×7000 NILs contained blocks of BT×642 DNA that partially or completely spanned a stay-green locus plus a variable amount of DNA flanking the target locus. The results of marker-assisted selection can be attributed to the stochastic nature of recombination and the limited availability of DNA markers at the start of this project. For example, the three DNA markers used for introgression of BT×642 DNA corresponding to *Stg2* were derived from one edge of this QTL and DNA adjacent to

the QTL. As a consequence, most of the RT×7000 NILs containing BT×642 corresponding to *Stg2* spanned only a portion of this locus (Fig. 2). Similarly, only a single DNA marker, Xtxs713 was used to identify BT×642 DNA introgressions corresponding to *Stg4* and therefore the resulting *Stg4* NILs contained BT×642 DNA that spanned only a portion of this QTL (Fig. 2). Nevertheless, the subset of RT×7000 NILs containing BT×642 DNA that span different portions of each stay-green QTL will be useful for further delimiting these loci in follow up experiments.

RT×7000 NILs containing BT×642 DNA spanning only *Stg1* (6078-1), *Stg2* (2219-3), *Stg3* (2290-19) or *Stg4* (6085-9) were identified among the original set of 34 NILs constructed during this project. NIL 6078-1 contained BT×642 DNA that completely spans *Stg1*. However, 2219-3, 2290-19, and 6085-9 NILs contained BT×642 DNA that spanned most, but not all, of the associated QTL. Fortunately, physiological analysis of these four RT×7000 NILs showed that each of these NILs included BT×642 alleles that could contribute to the stay-green trait. While it is likely that the BT×642 alleles contributing to the observed phenotypes correspond to *Stg1–Stg4*, all of these NILs contain BT×642 DNA outside of the regions previously identified as containing the QTL. This is not unexpected, as the location of the QTL is inherently uncertain since it relies heavily on the stochastic process of recombination, particularly in small mapping populations. Thus the true location of a particular QTL may be outside of, but linked to, the region identified as its location. Fine mapping studies are underway to confirm these findings and eventually to clone the genes involved.

NIL 2219-3 that contains BT×642 DNA from *Stg2* had the highest *GLAM* under terminal drought conditions among the NILs analysed relative to RT×7000 in both Experiments 1 and 2. Absolute and relative rates of leaf senescence were also lowest in *Stg2* among the NILs analysed compared with RT×7000 in both experiments. In addition, measurements of leaf greenness with a chlorophyll meter showed a clear trend for delayed onset and reduced rate of leaf senescence in the *Stg2* NIL relative to RT×7000. These results are consistent with prior analysis indicating that *Stg2* has the largest influence on the expression of the stay-green phenotype among the four major *Stg* loci identified in the RT×7000/BT×642 population (Subudhi *et al.*, 2000; Xu *et al.*, 2000). Analysis of the stay-green NILs also indicates that all four stay-green loci derived from BT×642 can contribute to the stay-green phenotype in the absence of the other stay-green loci and other portions of the BT×642 genome. For example, NIL 6078-1 containing BT×642 DNA from *Stg1*, exhibited (relative to RT×7000) lower absolute and relative rates of leaf senescence in Experiment 2, a trend for higher *GLAM* in Experiments 1 and 2 ( $P<0.01$ , LD only), and higher *SPAD* at anthesis in Experiment 2. NIL

2290-19 containing BT×642 DNA from *Stg3*, exhibited (relative to RT×7000) lower absolute rates of leaf senescence in Experiments 1 and 2, a trend for higher *GLAM* in Experiments 1 and 2, and a trend for higher *SPAD* at anthesis and delayed onset of leaf senescence in Experiment 2. NIL 6085-9 containing BT×642 DNA from *Stg4*, was assessed only in Experiment 2; however, this NIL exhibited (relative to RT×7000) a lower absolute rate of leaf senescence, a trend for lower relative rate of leaf senescence, a trend for higher *GLAM* under LD and HD, higher *SPAD* at anthesis ( $P < 0.01$ ), and a trend for delayed onset of leaf senescence.

The trend for delayed onset of leaf senescence exhibited by the *Stg2*, *Stg3*, and *Stg4* NILs in Experiment 2 supports earlier research by Borrell *et al.* (2000a) who found delayed onset of senescence in A35 hybrids (stay-green) compared with AQL39 hybrids (senescent) under a terminal water deficit. The lower rates of leaf senescence observed in the stay-green NILs, and in particular *Stg2*, also agree with earlier work by Borrell *et al.* (2000a). Furthermore, higher *SPAD* at anthesis in *Stg1* and *Stg4* NILs in Experiment 2 is consistent with previous studies showing higher specific leaf nitrogen at anthesis (Borrell and Hammer, 2000) and higher *SPAD* at anthesis (Borrell *et al.*, 2001) in A35 hybrids compared with AQL39 hybrids under a terminal water deficit.

The strong positive correlation ( $r^2=0.98$ ) observed between *SPAD* measured at 67 DAA and *SPAD* predicted at 67 DAA (*SPAD<sub>m</sub>*) suggests that the components of *SPAD<sub>m</sub>* (*SPAD<sub>a</sub>*, *Duration<sub>sen</sub>* and *Rate<sub>sen</sub>*) may provide insights into the functional basis of leaf senescence. The significant correlation ( $r = -0.75$ ) between *SPAD<sub>m</sub>* and rate of loss of *SPAD* (coefficient 'c') on the one hand, and the lack of correlation ( $r = 0.17$ ) between *SPAD<sub>m</sub>* and the onset of leaf senescence (coefficient 'd') on the other, indicates that 'rate' rather than 'onset' of leaf senescence was the more important component of stay-green in this study.

Further physiological studies of these individual NILs will enable the mechanisms causing stay-green to be identified for each of the four genomic regions alone (*Stg1*, *Stg2*, *Stg3*, or *Stg4*). NILs containing various combinations of *Stg1–Stg4* will also be studied, enabling the extent of gene interaction to be assessed for this trait. Ongoing fine-mapping studies should allow the key genes from each region to be identified.

## Acknowledgements

This research was supported by National Science Foundation Plant Genome Research Grant DBI-0321578 (PEK, RRK, and JEM), by the Texas Agricultural Experiment Station (PEK and JEM), by the USDA-ARS (RRK), by the Grains Research and Development Corporation Grant DAQ520 (AKB), and by the Queensland Department of Primary Industries and Fisheries (AKB and DRJ).

## References

- Ambler J, Morgan P, Jordan W. 1987. Genetic regulation of senescence in tropical grass. In: Thomson W, ed. *Plant senescence: its biochemistry and physiology*. Rockville, MD: American Society of Plant Physiologists, 43–53.
- Beavis W. 1994. The power and deceit of QTL experiments: lessons from comparative QTL studies. In: Wilkinson D, ed. *49th Annual corn and sorghum research conference*. Chicago, IL, 250–266.
- Boivin K, Deu M, Rami JF, Trouche G, Hamon P. 1999. Towards a saturated sorghum map using RFLP and AFLP markers. *Theoretical and Applied Genetics* **98**, 320–328.
- Borrell A, Hammer G, van Oosterom E. 2001. Stay-green: a consequence of the balance between supply and demand for nitrogen during grain filling. *Annals of Applied Biology* **138**, 91–95.
- Borrell AK, Hammer GL. 2000. Nitrogen dynamics and the physiological basis of stay-green in sorghum. *Crop Science* **40**, 1295–1307.
- Borrell AK, Hammer GL, Douglas ACL. 2000a. Does maintaining green leaf area in sorghum improve yield under drought? I. Leaf growth and senescence. *Crop Science* **40**, 1026–1037.
- Borrell AK, Hammer GL, Henzell RG. 2000b. Does maintaining green leaf area in sorghum improve yield under drought? II. Dry matter production and yield. *Crop Science* **40**, 1037–1048.
- Bowers JE, Abbey C, Anderson S, *et al.* 2003. A high-density genetic recombination map of sequence-tagged sites for *Sorghum*, as a framework for comparative structural and evolutionary genomics of tropical grains and grasses. *Genetics* **165**, 367–386.
- Bowers JE, Arias MA, Asher R, *et al.* 2005. Comparative physical mapping links conservation of microsynteny to chromosome structure and recombination in grasses. *Proceedings of the National Academy of Sciences, USA* **102**, 13206–13211.
- Buchanan CD, Lim S, Salzman RA, *et al.* 2005. *Sorghum bicolor*'s transcriptome response to dehydration, high salinity and ABA. *Plant Molecular Biology* **58**, 699–720.
- Buchanan-Wollaston V, Earl S, Harrison E, Mathas E, Navabpour S, Page T, Pink D. 2003. The molecular analysis of leaf senescence: a genomics approach. *Plant Biotechnology Journal* **1**, 3–22.
- Casa AM, Mitchell SE, Hamblin MT, Sun H, Bowers JE, Paterson AH, Aquadro CF, Kresovich S. 2005. Diversity and selection in sorghum: simultaneous analyses using simple sequence repeats. *Theoretical and Applied Genetics* **111**, 23–30.
- Cha K-W, Lee Y-J, Koh H-J, Lee B-M, Nam Y-W, Paek N-C. 2002. Isolation, characterization, and mapping of the stay green mutant in rice. *Theoretical and Applied Genetics* **104**, 526–532.
- Childs KL, Miller FR, Cordonnier-Pratt MM, Pratt LH, Morgan PW, Mullet JE. 1997. The sorghum photoperiod sensitivity gene, *Ma3*, encodes a phytochrome B. *Plant Physiology* **113**, 611–619.
- Crasta OR, Xu WW, Rosenow DT, Mullet J, Nguyen HT. 1999. Mapping of post-flowering drought resistance traits in grain sorghum: association between QTLs influencing premature senescence and maturity. *Molecular and General Genetics* **262**, 579–588.
- Dahlberg JA. 1992. Variation of  $^{14}\text{C}$  assimilate export and partitioning in reduced progressive senescent and senescent sorghums [*Sorghum bicolor* (L.) Moench] and the potential use of anatomical features as a genetic marker for variation in sorghum. PhD thesis, Texas A&M University.
- Dje Y, Heuertz M, Lefebvre C, Vekemans X. 2000. Assessment of genetic diversity within and among germplasm accessions in cultivated sorghum using microsatellite markers. *Theoretical and Applied Genetics* **100**, 918–925.

- Doggett H.** 1988. *Sorghum*. New York, NY: John Wiley.
- Duncan RR, Bockholt AJ, Miller FR.** 1981. Descriptive comparison of senescent and non-senescent sorghum genotypes. *Agronomy Journal* **73**, 849–853.
- Edwards GE, Franceschi VR, Voznesenskaya EV.** 2004. Single-cell C<sub>4</sub> photosynthesis versus the dual-cell (Kranz) paradigm. *Annual Review of Plant Biology* **55**, 173–196.
- Gleick PH.** 2003. Global freshwater resources: soft-path solutions for the 21st century. *Science* **302**, 1524–1528.
- Hausmann BIG, Hess DE, Seetharama N, Welz HG, Geiger HH.** 2002a. Construction of a combined sorghum linkage map from two recombinant inbred populations using AFLP, SSR, RFLP, and RAPD markers, and comparison with other sorghum maps. *Theoretical and Applied Genetics* **105**, 629–637.
- Hausmann BIG, Mahalakshmi V, Reddy BVS, Seetharama N, Hash CT, Geiger HH.** 2002b. QTL mapping of stay-green in two sorghum recombinant inbred populations. *Theoretical and Applied Genetics* **106**, 133–142.
- Henzell RG, Hare BR, Jordan DR, Fletcher DS, McCosker AN, Bunker G, Persley DS.** 2001. Sorghum breeding in Australia: public and private endeavours. In: Borrell AK, Henzell RG, eds. *Proceedings of the 4th Australian sorghum conference*. Kooralbyn, Australia.
- Jordan DR, Tao Y, Godwin ID, Henzell RG, Cooper M, McIntyre CL.** 2003. Prediction of hybrid performance in grain sorghum using RFLP markers. *Theoretical and Applied Genetics* **106**, 559–567.
- Kebede H, Subudhi PK, Rosenow DT, Nguyen HT.** 2001. Quantitative trait loci influencing drought tolerance in grain sorghum (*Sorghum bicolor* L. Moench). *Theoretical and Applied Genetics* **103**, 266–276.
- Khush GS.** 1999. Green revolution: preparing for the 21st century. *Genome* **42**, 646–655.
- Kim JS, Islam-Faridi MN, Klein PE, Stelly DM, Price HJ, Klein RR, Mullet JE.** 2005. Comprehensive molecular cytogenetic analysis of sorghum genome architecture; distribution of euchromatin, heterochromatin, genes and recombination in comparison to rice. *Genetics* **171**, 1963–1976.
- Klein PE, Klein RR, Cartinhour SW, et al.** 2000. A high-throughput AFLP-based method for constructing integrated genetic and physical maps: progress toward a sorghum genome map. *Genome Research* **10**, 789–807.
- Klein PE, Klein RR, Vrebalov J, Mullet JE.** 2003. Sequence-based alignment of sorghum chromosome 3 and rice chromosome 1 reveals extensive conservation of gene order and one major chromosomal rearrangement. *The Plant Journal* **34**, 605–621.
- Klein RR, Klein PE, Mullet JE, Minx P, Rooney WL, Schertz KF.** 2005. Fertility restorer locus *Rfl* of sorghum (*Sorghum bicolor* L.) encodes a pentatricopeptide repeat protein not present in the colinear region of rice chromosome 12. *Theoretical and Applied Genetics* **111**, 994–1012.
- Lin YR, Schertz KF, Paterson AH.** 1995. Comparative analysis of QTLs affecting plant height and maturity across the Poaceae, in reference to an interspecific sorghum population. *Genetics* **141**, 391–411.
- Ludlow MM, Muchow RC.** 1990. A critical evaluation of traits for improving crop yields in water-limited environments. *Advances in Agronomy* **43**, 107–153.
- McBee GG.** 1984. Relation of senescence, nonsenescence, and kernel maturity to carbohydrate metabolism in sorghum. In: Mughogho LK, ed. *Sorghum root and stalk diseases, a critical review*. Proceedings of the consultative group discussion of research needs and strategies for control of sorghum root and stalk diseases. Bellagio, Italy. 119–129.
- McBee GG, Miller FR.** 1982. Carbohydrates in sorghum culms as influenced by cultivars, spacing, and maturity over a diurnal period. *Crop Science* **22**, 381–385.
- McKeown FR.** 1978. *A land classification of the Hermitage Research Station*. Brisbane, Australia: Queensland Department of Primary Industries, Division of Land Utilisation.
- Melchinger AE, Utz HF, Schon CC.** 1998. Quantitative trait locus (QTL) mapping using different testers and independent population samples in maize reveals low power of QTL detection and large bias in estimates of QTL effects. *Genetics* **149**, 383–403.
- Menz MA, Klein RR, Mullet JE, Obert JA, Unruh NC, Klein PE.** 2002. A high-density genetic map of *Sorghum bicolor* (L.) Moench based on 2926 AFLP<sup>(R)</sup>, RFLP and SSR markers. *Plant Molecular Biology* **48**, 483–499.
- Menz MA, Klein RR, Unruh NC, Rooney WL, Klein PE, Mullet JE.** 2004. Genetic diversity of public inbreds of sorghum determined by mapped AFLP and SSR markers. *Crop Science* **44**, 1236–1244.
- Mullet JE, Klein RR, Klein PE.** 2001. *Sorghum bicolor*: an important species for comparative grass genomics and a source of beneficial genes for agriculture. *Current Opinion in Plant Biology* **5**, 118–121.
- Northcote KH.** 1974. *A factual key for the recognition of Australian soils*, 3rd edn. Glenside, SA: Australia: Rellim Technical Publication.
- Paran I, Zamir D.** 2003. Quantitative traits in plants: beyond the QTL. *Trends in Genetics* **19**, 303–306.
- Peng Y, Schertz KF, Cartinhour S, Hart GE.** 1999. Comparative genome mapping of *Sorghum bicolor* (L.) Moench using an RFLP map constructed in a population of recombinant inbred lines. *Plant Breeding* **118**, 225–235.
- Pereira MG, Lee M.** 1995. Identification of genomic regions affecting plant height in sorghum and maize. *Theoretical and Applied Genetics* **90**, 380–388.
- Pratt LH, Liang C, Shah M, et al.** 2005. Sorghum expressed sequence tags identify signature genes for drought, pathogenesis, and skotomorphogenesis from a milestone set of 16 801 unique transcripts. *Plant Physiology* **139**, 869–884.
- Price HJ, Dillon SL, Hodnett G, Rooney WL, Ross L, Johnston JS.** 2005. Genome evolution in the genus *Sorghum* (Poaceae). *Annals of Botany* **95**, 219–227.
- Rosenow DT.** 1983. Breeding for resistance to root and stalk rots in Texas. *Sorghum root and stalk rots, a critical review*. Patancheru, AP, India: ICRISTAT, 209–217.
- Rosenow DT, Clark LE.** 1981. Drought tolerance in sorghum. In: Loden HD, Wilkinson D, eds. *Proceedings of the 36th annual corn and sorghum industry research conference*, Chicago, IL. 18–30.
- Rosenow DT, Clark LE.** 1995. Drought and lodging resistance for a quality sorghum crop. In: Proceedings of the 50th annual corn and sorghum industry research conference, Chicago, IL. 82–97.
- Salzman RA, Brady JA, Finlayson SA, et al.** 2005. Transcriptional profiling of sorghum induced by methyl jasmonate, salicylic acid, and aminocyclopropane carboxylic acid reveals cooperative regulation and novel gene responses. *Plant Physiology* **138**, 352–368.
- Sanchez AC, Subudhi PK, Rosenow DT, Nguyen HT.** 2002. Mapping QTLs associated with drought resistance in sorghum (*Sorghum bicolor* L. Moench). *Plant Molecular Biology* **48**, 713–726.
- Subudhi PK, Magpantay G, Rosenow DT, Nguyen HT.** 1999. Mapping and marker-assisted selection to improve stay green trait in sorghum for drought tolerance. In: Ito O, O'Toole J, Hardy B, eds. *Genetic improvement of rice for water-limited environments*.

- Los Baños, Philippines: International Rice Research Institute, 183–191.
- Subudhi PK, Rosenow DT, Nguyen HT.** 2000. Quantitative trait loci for the stay green trait in sorghum (*Sorghum bicolor* L. Moench): consistency across genetic backgrounds and environments. *Theoretical and Applied Genetics* **101**, 733–741.
- Tao YZ, Hardy A, Drenth J, Henzell RG, Franzmann BA, Jordan DR, Butler DG, McIntyre CL.** 2003. Identification of two different mechanisms for sorghum midge resistance through QTL mapping. *Theoretical and Applied Genetics* **107**, 116–122.
- Tao YZ, Henzell RG, Jordan DR, Butler DG, Kelly AM, McIntyre CL.** 2000. Identification of genomic regions associated with stay green in sorghum by testing RILs in multiple environments. *Theoretical and Applied Genetics* **100**, 1225–1232.
- Tao YZ, Jordan DR, Henzell RG, McIntyre CL.** 1998. Construction of a genetic map in a sorghum recombinant inbred line using probes from different sources and its comparison with other sorghum maps. *Australian Journal of Agricultural Research* **49**, 729–736.
- Thomas H, Howarth CJ.** 2000. Five ways to stay green. *Journal of Experimental Botany* **51**, 329–337.
- Thomas H, Smart CM.** 1993. Crops that stay green. *Annals of Applied Biology* **123**, 193–219.
- Tuinstra MR, Ejeta G, Goldsbrough P.** 1998. Evaluation of near-isogenic sorghum lines contrasting for QTL markers associated with drought tolerance. *Crop Science* **38**, 835–842.
- Tuinstra MR, Grote EM, Goldsbrough PB, Ejeta G.** 1996. Identification of quantitative trait loci associated with pre-flowering drought tolerance in sorghum. *Crop Science* **36**, 1337–1344.
- Tuinstra MR, Grote EM, Goldsbrough PB, Ejeta G.** 1997. Genetic analysis of post-flowering drought tolerance and components of grain development of *Sorghum bicolor* (L.) Moench. *Molecular Breeding* **3**, 439–448.
- van Oosterom EJ, Jayachandran R, Bidinger FR.** 1996. Diallel analysis of the stay-green trait and its components in sorghum. *Crop Science* **36**, 549–555.
- Vos P, Hogers R, Bleeker M, Reijans M, van de Lee T, Hornes M, Frijters A, Pot J, Peleman J, Kuiper M.** 1995. AFLP: a new technique for DNA fingerprinting. *Nucleic Acids Research* **23**, 4407–4414.
- Walulu RS, Rosenow DT, Wester DB, Nguyen HT.** 1994. Inheritance of the stay green trait in sorghum. *Crop Science* **34**, 970–972.
- Woodfin CA, Rosenow DT, Clark LE.** 1998. Association between the stay-green trait and lodging resistance in sorghum. In: *Agronomy abstracts*. Madison, WI: ASA, 102.
- Xu W, Subudhi PK, Crasta OR, Rosenow DT, Mullet JE, Nguyen HT.** 2000. Molecular mapping of QTLs conferring stay-green in grain sorghum (*Sorghum bicolor* L. Moench). *Genome* **43**, 461–469.
- Yoshida S.** 2003. Molecular regulation of leaf senescence. *Current Opinion in Plant Biology* **6**, 79–84.